Catalysis Communications 186 (2024) 106802

Contents lists available at ScienceDirect

Catalysis Communications

journal homepage: www.elsevier.com/locate/catcom

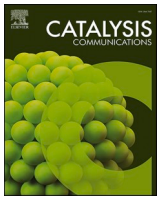

Stability, deactivation and regeneration study of a newly developed HZSM-5 and Ni-doped HZSM-5 zeolite catalysts for ethanol-to-hydrocarbon conversion

Ifeanyi Michael Smarte Anekwe [a,*], Maggie Chetty [b], Lindiwe Khotseng [c], Sammy Lewis Kiambi [d], Lakesh Maharaj [e], Bilainu Oboirien [f], Yusuf Makarfi Isa [a]

[a] School of Chemical and Metallurgical Engineering, University of the Witwatersrand, Johannesburg 2050, South Africa
[b] Department of Chemical Engineering, Cape Peninsula University of Technology, Cape Town 7535, South Africa
[c] Department of Chemistry, University of The Western Cape, Bellville 7535, South Africa
[d] Department of Chemical and Metallurgical Engineering, Vaal University of Technology, Vanderbijlpark 1911, South Africa
[e] uMngeni-uThukela Water, P. O. Box 9, Pietermaritzburg 3201, South Africa
[f] Department of Chemical Engineering Technology, University of Johannesburg, Johannesburg, South Africa

ARTICLE INFO

Keywords:
Catalyst
Ethanol
Regeneration
Stability
ZSM-5

ABSTRACT

This work investigates the stability and regeneration of HZSM-5 and Ni/HZSM-5 catalysts in the ethanol-to-hydrocarbon conversion. The catalysts were characterised using different techniques and evaluated at 623 K and 7 h^{-1} for 96 h TOS with two regeneration cycles. HZSM-5 showed high stability with 100% ethanol conversion, while Ni/HZSM-5 catalysts maintained 100% stability for 48 h before dropping. Regenerated catalysts were comparable to the originals in terms of product distribution, stability, and performance. HZSM-5 preferred BTX, while Ni-doped catalysts favoured C_5-C_8, C_9-C_{12}, and C_{12}+ synthesis. The regeneration process restored catalytic activity, especially for the Ni-doped catalysts, extending their life and reducing replacement costs.

1. Introduction

The development of substitutes for petroleum has become a pressing issue worldwide due to the impending petroleum crisis and the need to reduce CO_2 emissions. One promising option is biomass, a renewable resource that is both abundant and carbon emissions-free. Biomass can be utilised directly to generate heat and electricity. It can also be converted thermochemically or biochemically into combustible liquids such as bio-oils, methanol, and ethanol, as well as gases like methane and hydrogen [1]. The fermentation of biomass feedstocks, such as sugarcane, sugar beets, and starch crops, is a widely utilised biochemical conversion process, with bioethanol being one of the most easily produced end products. The global bioethanol production in 2020 was 29.66 billion litres [2]. While bioethanol is commonly used as fuel or fuel additive for motor vehicles, recent attention has been given to its use as a feedstock for the chemical industry, particularly in producing ethylene through catalytic dehydration of ethanol.

Zeolites, a family of catalysts widely used in petroleum refining and fluid catalytic cracking (FCC), are useful in converting methanol and ethanol to hydrocarbons. Zeolite HZSM-5, developed by Mobil Oil Corporation in 1972, has been a widely used catalytically active material for converting methanol and ethanol to hydrocarbons due to its effectiveness as an additive in FCC catalysts or hydrocracking [3]. Due to its frequent use in these processes, a vast array of distinct post-synthetic modification possibilities are available for zeolite HZSM-5. Post-synthesis procedures contribute to tuning its activity and selectivity, respectively, as well as its stability and regenerability. Additionally, the synthesis process results in several variations in the Si/Al ratio, further contributing to the catalyst's versatility [4–7].

The process of ethanol-to-hydrocarbon (ETH) conversion is a complex one that involves several types of chemical interactions. The latest research has delved into the reactions that Lewis and Bronsted acid sites catalyse. After ethanol is rapidly and almost entirely dehydrated, producing ethene and diethyl ether, a process referred to as "hydrocarbon pool" emerges. This process involves a series of carbocation-based events, including oligomerisation, cracking, cyclisation, isomerisation, and hydride transfer reactions. These reactions occur on various hydrocarbon species located on different acid sites in the active surface of

* Corresponding author.
E-mail address: anekwesmarte@gmail.com (I.M.S. Anekwe).

https://doi.org/10.1016/j.catcom.2023.106802
Received 17 August 2023; Received in revised form 31 October 2023; Accepted 12 November 2023
Available online 15 November 2023

the porous catalyst material, resulting in the formation of a hydrocarbon pool of homologating compounds [8–11]. To achieve higher levels of selectivity in the ETH process, researchers have explored the possibility of modifying ZSM-5 zeolites by adding metals such as Fe or W and La [12]. Studies have been carried out to enhance the catalyst's stability since zeolites undergo irreversible deactivation throughout the reaction. One promising approach has been to incorporate phosphorus into the ZSM-5 zeolites, which can improve their hydrothermal stability. Recent studies have shown that phosphorus-modified ZSM-5 (P-ZSM-5) catalysts have improved selectivity for propylene synthesis and strong catalytic stability [13–15]. Despite these promising results, it is still not entirely clear how the addition of phosphorus influences the ZSM-5 catalysts during the conversion of ethanol to hydrocarbons. Further research is needed to understand this process's complex interactions and chemical pathways fully.

The ZSM-5 catalyst has proven to be a viable option for hydrocarbon reactions. However, due to catalyst coking, zeolites tend to experience rapid deactivation, necessitating their routine regeneration throughout the fluid catalytic cracking (FCC) process to restore their catalytic performance. Although coking with feedstocks can deactivate zeolites, oxidative treatments can bring them back to life [16]. This process has been the subject of extensive research, and a dilute air stream is a standard, effective method for coke removal from zeolites. This air stream is used to control the rate of oxidation, which in turn limits the exothermic processes and steam generation that might result in irreversible dealumination of the catalyst. It is worth noting that although general techniques for coke removal from zeolites can be utilised for various kinds of reactions, the type of coke is determined by the feedstock from which it originates. The extent of regeneration is influenced by the catalyst and reaction conditions employed to produce the coke [17]. Therefore, protocols for regeneration must be designed for each application, considering factors such as feedstock, catalyst, process conditions, etc. [18].

Benito, et al. [19] studied the regeneration of ZSM-5, utilised in converting methanol to gasoline. They found the catalyst susceptible to thermal destruction. Still, it could be reactivated at 823 K in air, provided it had been exposed to the same temperature before its initial activity was determined. Other studies have also been conducted on the regeneration of ZSM-5, which has been utilised for in-situ and ex-situ biomass conversion to hydrocarbons. The temperatures ranged from 723 to 973 K, and the number of reaction cycles ranged from 1 to 10 [20,21]. Williams and Horne [22] discovered that the efficiency of an HZSM-5 zeolite in converting oils produced by biomass pyrolysis into aromatic compounds decreased after the zeolite had been regenerated up to five times. To regenerate the spent catalyst, it was extracted from the reactor and subjected to air heating at 823 K for eight hours in an oven. Carlson, et al. [20] studied a ZSM-5 catalyst for ten reaction/regeneration cycles, with regeneration performed for three hours in the air. They discovered a modest reduction in low-temperature acid sites, characterised by ammonia temperature-programmed desorption. They also found that metals from the biomass were deposited on the catalysts despite no investigation or optimisation of the regeneration process being reported. In their research, Paasikallio, et al. [21] carried out catalyst regeneration at temperatures ranging from 923 to 943 K. Over 100 h, they observed a slight shift in the product's composition. They reported that catalyst deactivation was limited but noticeable, with negligible loss of total surface area and a decrease of approximately 30% in the micropore volume [21].

The previous studies that have been conducted on catalyst regeneration have primarily focused on commercial ZSM-5 for low alcohol conversion to olefins or synthesised ZSM-5 for biomass or bio-oil conversion into hydrocarbons. In addition to the aforementioned studies, research has also explored the addition of phosphorus to improve catalyst stability. However, it is essential to note that while this approach may enhance catalyst stability, it may not necessarily improve the selectivity towards target products. As a result, there has not been a sufficient study on the stability and regeneration of newly fabricated ZSM-5 zeolite catalysts, specifically in converting ethanol to liquid hydrocarbons. In this study, we seek to address this gap in the literature by investigating the stability and deactivation of newly synthesised ZSM-5 (Si/Al = 40) and Ni-doped ZSM-5 zeolite catalysts without the addition of phosphorus in the conversion of ethanol to liquid hydrocarbons. Furthermore, we aim to compare the performance of unmodified and Ni-doped ZSM-5 catalysts to explore the effect of transition metals on catalyst stability during the ethanol-to-hydrocarbon (ETH) process. In addition, we investigated catalyst deactivation due to coke deposition and regeneration to determine its impact on the stability and product distribution of both ZSM-5 and Ni/HZSM-5 catalysts. Through these investigations, we aim to provide valuable insights into the design of more stable and effective catalysts for the conversion of ethanol to liquid hydrocarbons, with the potential to advance the field of sustainable bioenergy production.

2. Materials and method

2.1. Materials

The following chemicals were utilised for this study: silica source: sodium silicate solution, aluminium source: aluminium sulfate, organic template: tetrapropyl ammonia bromide, sodium hydroxide (97%), sulfuric acid (98% conc.), ammonium nitrate. Nickel nitrate precursor was employed for the introduction of nickel. Ethanol was employed as the feedstock for the catalytic test, and all chemicals were obtained from Sigma-Aldrich. A Teflon-lined stainless-steel hydrothermal reactor of 200 mL was used for the catalyst synthesis.

2.2. Methods

The hydrothermal catalyst synthesis technique was used to prepare the ZSM-5 catalyst support according to our previous work [23], with a batch formula of $10Na_2O$: $40SiO_2$: $1.0Al_2O_3$: 10.5TPABr: $3740.6H_2O$. Three solutions were prepared, mixed, and agitated vigorously for 6 h in the following order: Solution 1 (consisting of a silica source and NaOH dissolved in deionised water), solution 2 (created by dissolving tetrapropylammonium bromide in deionised water), and solution 3 (containing deionised water with aluminium sulfate dissolved in it). After mixing and stirring vigorously for 1 h, the pH of the gel was adjusted with sulfuric acid before ageing for 12 h and then subjected to hydrothermal crystallisation at 453 K for 24 h. The resulting Na-ZSM-5 was ion-exchanged (to NH_4-ZSM-5) under reflux with 1 M of NH_4NO_3 solution at 10 mL/g catalyst at 353 K for 3 h and calcined at 823 K to obtain the HZSM-5 catalyst (denoted as Z5). Transition metal (Ni) was incorporated at 0.5 wt% via incipient impregnation to produce the Ni-modified HZSM-5 catalyst with the designation NiZ.

The catalytic stability and performance of Z5 and NiZ were studied at a temperature of 350 °C and weight hourly space velocities (WHSV) of 7 h^{-1} for 96 h (with 8 h of sampling) in the conversion of ethanol into hydrocarbons. Glass beads and glass wool were used as structural support for the catalyst bed, and an HPLC pump was used to introduce the feedstock into the reactor after the initial activation of the catalyst at 400 °C. Product selectivity (Si) and conversion (X) were calculated based on the work of Sun, et al. [24].

2.2.1. Catalyst characterisation and product analysis

The zeolites' crystalline phase was analysed using a Bunker D2 Phase Diffractometer with Cu—K1 radiation and a 2° per minute scanning rate for powder X-ray diffraction. Functional groups were identified through Perkin Elmer Fourier Transform-Attenuated Total Reflectance - Infrared Spectrometer Sprecrum-2 at 4000–400 cm^{-1}.

Scanning electron microscopy was used to observe the morphologies of the samples (ZEISS Sigma 300 VP), while particle size distribution (PSD) was determined by dynamic light scattering analysis (DPSA) using

a Malvern Masterizer 2000 instrument. The sample was dispersed in distilled water and subjected to analysis with a He—Ne laser. The surface area and porous properties of the ZSM-5 zeolites were assessed using an N_2 adsorption–desorption analyser. Prior to the measurement, the zeolites were degassed by heating them to 573 K for ten hours.

The elemental composition of transition metals in the catalyst was determined through Energy dispersive X-ray spectroscopy (Oxford Instruments x-act PentaFET Precision ESD) and Panalytical X-ray fluorescence spectrometer was used to determine the elemental composition of the nickel metal in the doped catalys.

Ammonia temperature-controlled desorption was carried out using a chemisorption analyser (NH_3-TPD, AutoChem II 2920). To eliminate the adsorbed water, a sample of approximately 100 mg and a He flow rate of 40 mL/min was heated to 573 K at a rate of 10 °C per minute for two hours. After lowering the temperature to 373 K, NH_3 replaced He for 20 min. Finally, the sample was heated to 873 K at a rate of 283 K per minute, and the desorption NH_3 signal was obtained using a TCD detector.

HZSM-5 and Ni/HZSM-5 catalysts, initially labelled as Z5 and NiZ, were regenerated after 96 h on-stream by exposing them to an 80 mL/min airflow at 823 K for 5 h. The regenerated catalysts were designated Z5-R1 and NiZ-R1 for the first regeneration (R1) and Z5-R2 and NiZ-R2 for the second (R2).

Thermal characteristics and differential thermal analysis (DTA) of the used catalyst were assessed via Thermo gravimetric analysis, TGA (TA Instruments Q50, USA) to observe the extent of coke deposition post-reaction. The samples underwent heating in a nitrogen stream from ambient temperature to 200 °C with a ramp rate of 15 °C/min and a flow rate of 50 mL/min to eliminate unbound volatile materials and moisture. Afterwards, the flow of N_2 gas was substituted with airflow and heated to 800 °C with the same flow rate.

Liquid HCs were analysed using a YL6500 gas chromatograph (GC) system. The sample was injected at a temperature of 313 K. The column was then heated at a rate of 276 K/min to 323 K and maintained for 3 min. Next, it was heated at 275 K/min to 333 K and held for a minute. Subsequently, it was heated at a rate of 278 K/min to 473 K and held for a minute. Finally, the column was further heated to 588 K at a rate of 288 K/min and then maintained at that temperature for 5 min. The findings of the GC analysis are presented based on the peak area distribution.

3. Results and discussion

3.1. Catalyst characterisation of pure and regenerated catalysts

3.1.1. XRD - phase identification

The XRD pattern of the as-synthesised sample indicates that ZSM-5 has the same single crystalline phase as the standard ZSM-5 (JCPDS No. 96–154-0268) presented by the International Centre for Diffraction Data (ICDD). The standard ZSM-5 has an orthorhombic crystal system and is characterised by space group Pnma (#62) – a centrosymmetric with 8-point inversion per unit cell attributed to the orthorhombic space group [25,26], with lattice constants: a = 20.0480 Å, b = 19.8840 Å and c = 13.3520 Å. Fig. 1a shows that the most characteristic peaks of pure and modified HZSM-5 are found at 2θ = 7–9° and 23–25° [27–29]. Distinctive diffraction peaks were observed at 7.97°, 8.88°, 14.81°, 23.14°, 24.00° and 24.49° assigned to reflective planes (101), (020), (301), (501), (303) and (133) of the MFI framework of the ZSM-5 catalyst, indicating that the addition of Ni into ZSM-5 did not modify the framework of the material [28]. No discernible peaks of Ni oxide in the XRD pattern were detected, indicating that the Ni content was present in small quantities and that there was no significant aggregation of metal, suggesting a homogeneous dispersion of Ni species on the ZSM-5 support catalyst [30,31].

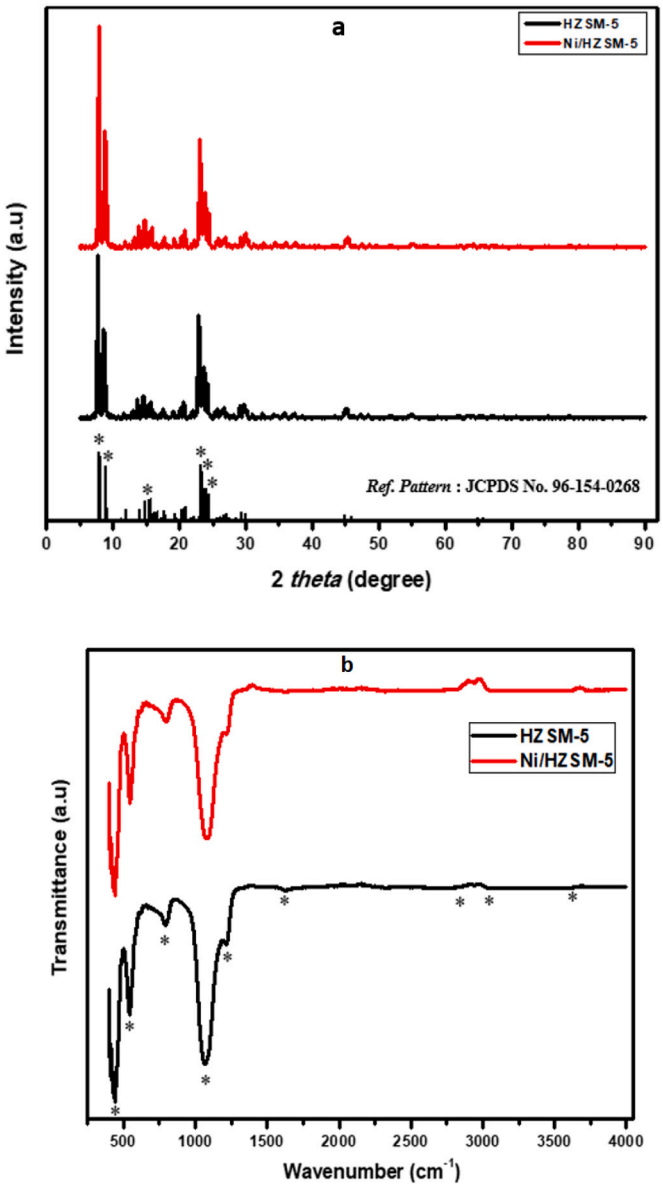

Fig. 1. Phase (a) and functional groups (b) identification of as-synthesised Z5 and NiZ catalysts.

3.1.2. FTIR - identification of functional groups

Fig. 1b presents the FT-IR spectrum of the as-synthesised and Ni/HZSM-5. The peak at 440 cm^{-1} corresponds to the tetrahedron units of SiO_4 and AlO_4, while the bands around 791 and 1064 cm^{-1} are associated with the symmetric stretching of the internal connections of the tetrahedrons (Si–O–Si linkage) [32]. The 543 cm^{-1} band is attributed to the five-membered ring of the pentasil zeolite framework, while the asymmetric stretching vibration of the T-O band at 1218 cm^{-1} (T = Si or Al) is assigned to external connections between TO_4 tetrahedral and is a framework-sensitive IR band of the ZSM-5 zeolite [33,34]. The peak at 3646 cm^{-1} corresponds to the silanol groups of Si-OH. Additionally, the peaks arising from the use of tetrapropylammonium bromide as a structural directing agent (SDA) precursor can be found at 2927 cm^{-1} for the methyl group (-CH_3) band and 2849 cm^{-1} for the methylene group (-CH_2) band [35,36]. A peak at 1633 cm^{-1} indicates the stretching bending of water molecules that have been adsorbed. The absorption peak around 440 cm^{-1} can also be associated with the SiO-bending vibrations of the SiO4 internal tetrahedral [37]. Finally, in agreement with the XRD result, no visible peak of Ni-oxide was observed on the FTIR

spectra, which suggests a low concentration of Ni species incorporated in the parent catalyst.

3.1.3. Morphological properties

The surface structures of HZSM-5 and Ni/HZSM-5 catalysts were examined using a scanning electron microscope, and the resulting SEM images are presented in Fig. 2. The Ni-loaded sample's micrograph shows that the zeolite's morphology remains unchanged after Ni impregnation. The EDX spectrum reveals the presence of nickel loading. High magnification SEM images reveal the aggregation of nanosized crystals forming microspheres, with similar morphologies to prismatic crystals ranging in size from approximately 100 to 800 nm in length. These prismatic and spheroid-like morphology nanocrystals are tightly packed. The surface morphology of unmodified HZSM-5 appears smoother than metal-modified HZSM-5, as introducing metal species leads to micro-blocks composed of many small nanosized primary ZSM-5 particles. The primary particle size was determined to be 4.35 μm using a particle size analyser, and the addition of Ni metal resulted in a 0.7 μm increase in particle size. The inset of Fig. 4 shows that the particle size distribution for HZSM-5 and Ni/HZSM-5 ranges from 0.5 to 100 and 0.4 to >100 μm, respectively. The Ni/HZSM-5 exhibits a bimodal particle distribution, which may have been induced by initial size differences or one distinct phase of accelerated growth for one portion of the particle population [38,39]. Moreover, the nucleation of new particles, which caused the initial peak in the size distribution, could partly elucidate the origin of the bimodal particle size distributions. Additional processes, such as the break-up of large particles, various sources of particles, ageing and variable growth patterns within the system, subsequently lead to the second peak, the accumulation mode [40,41]. The XRF result revealed the presence of NiO which consist of 0.54 wt% Ni species.

3.1.4. Textural properties of pure and regenerated catalysts

Adsorption plays a crucial role in heterogeneous catalysis as it activates the chemical bonds of adsorbed reactants. The N_2-adsorption isotherm of ZSM-5-MS indicates a hysteresis loop (type IV isotherm) at relative pressure P/P_0 of 0.4–1.0, confirming the presence of mesopores (Fig. 3) attributable to intercrystalline voids between the French fries-like crystals [42,43]. The isotherms of HZSM-5 and doped catalysts

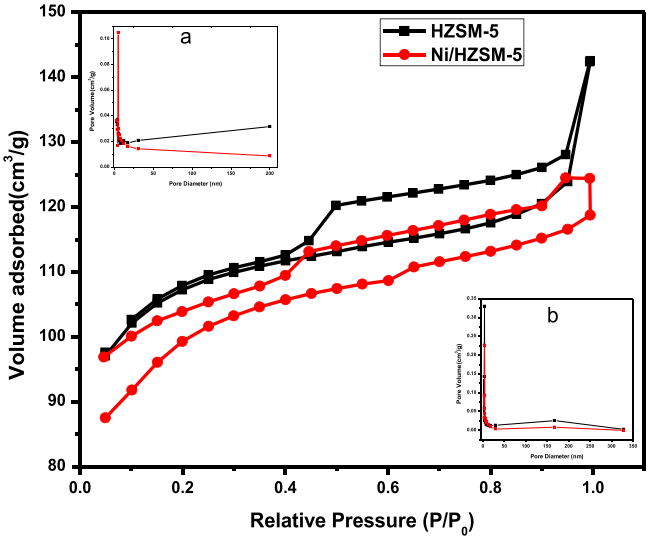

Fig. 3. N_2 adsorption-desorption isotherm results; Inset: BJH pore distribution for adsorption (a) and desorption (b) of the unmodified and Ni-doped HZSM-5 catalysts.

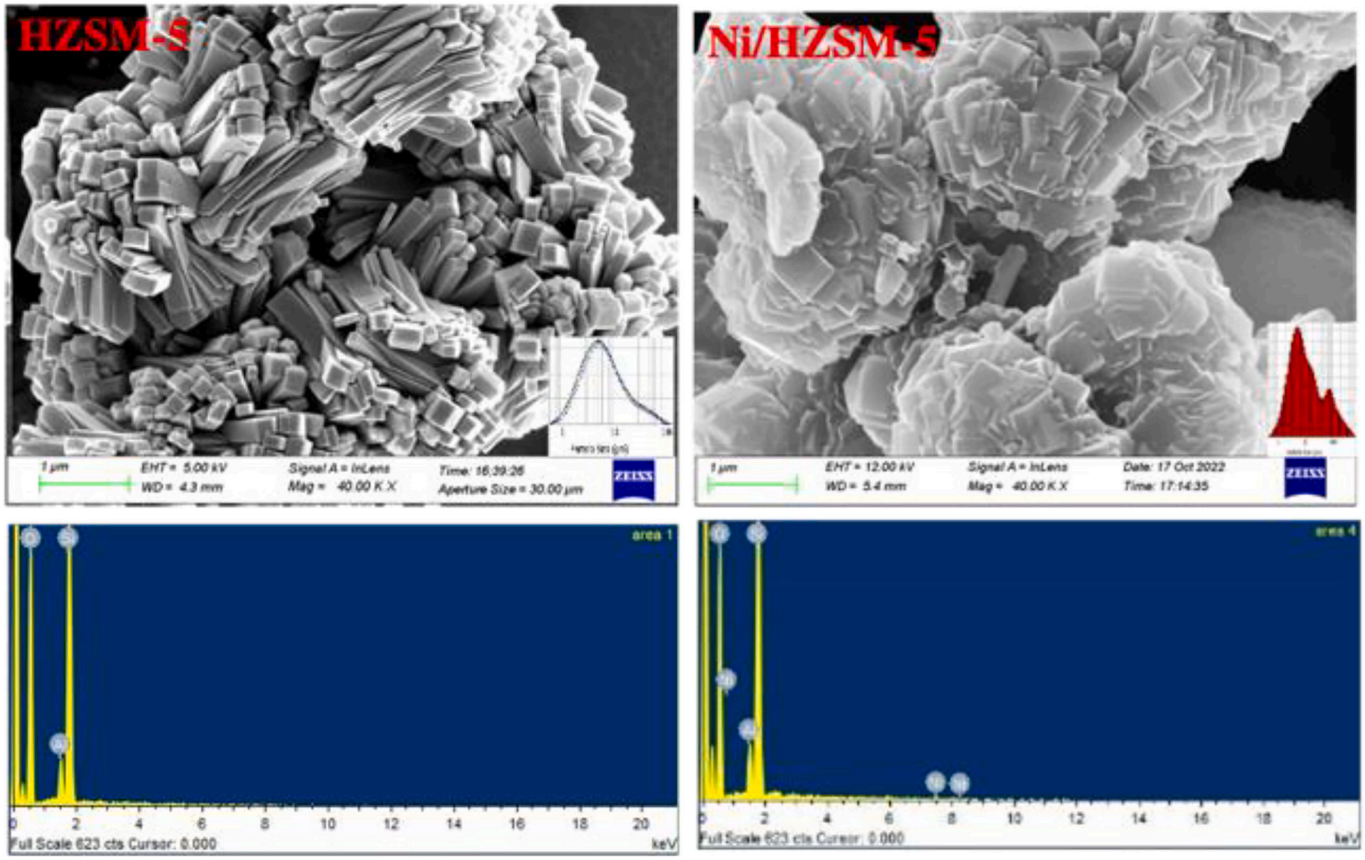

Fig. 2. SEM-EDS and PDS (inset) of the unmodified and Ni-doped HZSM-5.

show an increase in the adsorbed volume with p/p_0, with the adsorbed volume decreasing as Ni is incorporated. The pore size distribution (insets Fig. 5a and 5b) reveals prominent peaks at around 5 nm, with a tail up to 12 nm, indicating significant mesopores for zeolite application [43]. Moreover, the bare and Ni-modified ZSM-5 produced here exhibit a hierarchical porous structure (micro-meso-macroporous), providing additional insights into the peculiar pore structure of the zeolite. The BET surface areas of HZSM-5 and Ni/HZSM-5 are 397.47 and 381.36 $m^3 g^{-1}$, respectively. All samples have large surface areas, indicating the successful preparation of bare and Ni-modified ZSM-5 (Table 1). However, Ni-modified samples show slightly less surface area due to metal particle agglomeration and pore blockage [44]. Greater surface area facilitates HC reactions and enhances catalytic performance [44]. The introduction of Ni to the catalyst framework results in agglomerations, as observed in the SEM micrographs. The presence of Ni species reduces the surface area, total pore volume, and average pore diameter (APD) of the Ni-doped catalysts. Specifically, V_{total} and APD decrease from 0.221 $cm^3 g^{-1}$ and 2.224 nm, respectively, for unmodified HZSM-5, to 0.199 $cm^3 g^{-1}$ and 2.024 nm, respectively, for Ni/HZSM-5. The characterisation of the regenerated catalysts presented in the supplementary section shows that the physicochemical properties of the catalyst were preserved after regeneration.

The textural properties of the regenerated catalysts were studied after the regeneration process. The regenerated ZSM-5 and Ni/HZSM-5 catalysts have a considerable surface area (308.2 and 295.4 m^2/g, respectively) (Table 1), indicating that the regeneration process successfully preserved the overall porous structure of the catalysts. However, it should be noted that the surface area of the regenerated catalysts decreased slightly compared to the pure catalysts. In addition, the surface area of the unmodified catalysts was larger than that of the Ni doped catalysts due to the presence of Ni species, which may affect the accessibility of the active sites and limit the available surface area for adsorption and reaction. Notably, the regeneration process may result in the loss of active sites and structural changes in the catalyst, resulting in a reduction in surface area. In addition, the presence of coke deposits and other carbonaceous species, often formed during the catalytic reaction and accumulating on the catalyst surface, can contribute to the reduction in surface area. However, despite the reduction in surface area and average pore diameter, the total pore volume of the regenerated catalysts increases in contrast to the pure catalysts. This increase can be attributed to the formation of mesopores during the regeneration process. The regeneration process, which often involves high-temperature treatments, can lead to the restructuring of the catalyst and the formation of mesopores. These mesopores can contribute to the total pore volume of the catalyst, compensating for the decrease in surface area and average pore diameter. The increase in mesopores in the regenerated catalysts can have important implications for the improved catalytic performance of the regenerated catalysts. Mesopores can provide improved diffusion pathways for reaction molecules and enhance mass transport within the catalyst, leading to better accessibility of active sites and potentially improving catalytic activity and selectivity. This result agrees with previous studies [45,46].

Table 1
Textural properties of pure and regenerated catalysts.

Catalysts	S_{BET} (m^2/g)	V_{total} ($cm^3 g^{-1}$)	V_{meso} ($cm^3 g^{-1}$)	V_{macro} ($cm^3 g^{-1}$)	Avg pore dia. (nm)	Volume@STP ($cm^3 g^{-1}$)
HZSM-5	397.47	0.706	0.678	0.029	2.224	109.94
HZSM-5 (R)	308.16	0.681	0.664	0.017	2.61	101.69
Ni/HZSM-5	381.36	0.590	0.582	0.008	2.024	104.61
Ni/HZSM-5 (R)	295.39	0.697	0.663	0.034	2.66	97.70

3.1.5. NH_3-TPD results

The acidic properties of the unmodified and the Ni-doped catalysts were investigated through NH_3-TPD analysis (Table 2), where all samples showed a three-peak pattern at different temperature ranges: 100–300 °C, 300–500 °C, and 500–700 °C. These peaks corresponded to weak acid, moderate (moderately strong) acid, and strong acid sites, respectively. The weak acid sites (Lewis acid sites, LAS) were associated with silanol and end-chain hydroxyl groups, while the strong acid sites (Bronsted acid sites, BAS) were attributed to bridging hydroxyl between Si and Al in the zeolite framework [47]. The results demonstrated that after Ni addition, the weak acidity of ZSM-5 increased while the moderate and strong acidity decreased, with a shift in peak temperatures towards higher values due to the interaction between Ni species and HZSM-5. Introducing Ni species into the HZSM-5 catalyst resulted in a 10.4% increase in the low-temperature desorption bands. This led to an elevation in the number of LAS for the Ni/HZSM-5 catalyst, rising from 0.95 mmol/g NH_3 at 198 °C for the unmodified HZSM-5 to 1.06 mmol/g at 190 °C. This rise in LAS can be attributed to the formation of corresponding oxides, such as NiO, which act as LAS, increasing the number of weak acid sites [48]. A slight decrease of 6.8% was observed for the moderately strong acid sites, bringing the value down to 0.69 mmol/g for the Ni-doped catalysts. In contrast, a considerable decrease (41.7%) was observed for the strong acid sites, accompanied by a corresponding decrease in BAS. The total acidity increased by 2.8%, primarily due to increased LAS. The presence of metal ions in the zeolite framework may lead to substituting some acidic protons responsible for strong acid sites, decreasing their BAS. This ion exchange process between the metal ions and the acidic protons contributes to the observed decrease in strong acid sites [49].

3.2. Catalyst stability in ethanol conversion

Catalyst stability, Ethanol conversion, and product distribution were studied at a temperature of 623 K and a WHSV of 7 h^{-1}. It involved three cycles of ethanol conversion, each consisting of 96 h of time on stream (TOS) and two regenerations. The first cycle used as-synthesised or pure catalysts (Z5 and NiZ for the pure and Ni-modified ZSM-5 catalyst) for ethanol conversion (X %). After the first cycle, the catalysts were regenerated (first regeneration cycle, R1), denoted as Z5-R1 and NiZ-R1, and utilised for the second cycle of ethanol conversion. Following the second cycle, the catalysts were regenerated (second regeneration cycle, R2), denoted as Z5-R2 and NiZ-R2, and used for the third conversion cycle.

Fig. 4a and b show the conversion of ethanol and phase selectivity for each catalyst among the gaseous and liquid products. Aromatics (BTX: benzene, toluene, xylenes), C_5-C_8, and C_9+ hydrocarbons were the main liquid products, and their selectivity changed over time on stream. Ethanol conversion remained constant at approximately 100% for Z5 catalysts, while Ni-doped catalysts, NiZ, showed a decline in ETH conversion after 48 h on stream. The decline in conversion can be attributed to the addition of Ni species, which increases the acid site concentration, making the catalyst more susceptible to coking and leading to catalyst

Table 2
NH_3-TPD Results for HZSM-5 and Ni/HZSM-5.

Catalysts	Peak Temp (°C)			Acidity conc. (mmol NH_3/g)			
	L.T.	M.T.	H.T.	Weak	Moderate	Strong	Total acidity
HZSM-5	198	419	686	0.95	0.74	0.024	1.714
Ni/HSM-5	190	435	688	1.06	0.69	0.014	1.764

L.T – Low temperature, M.T – Medium temperature, H.T – High temperature.

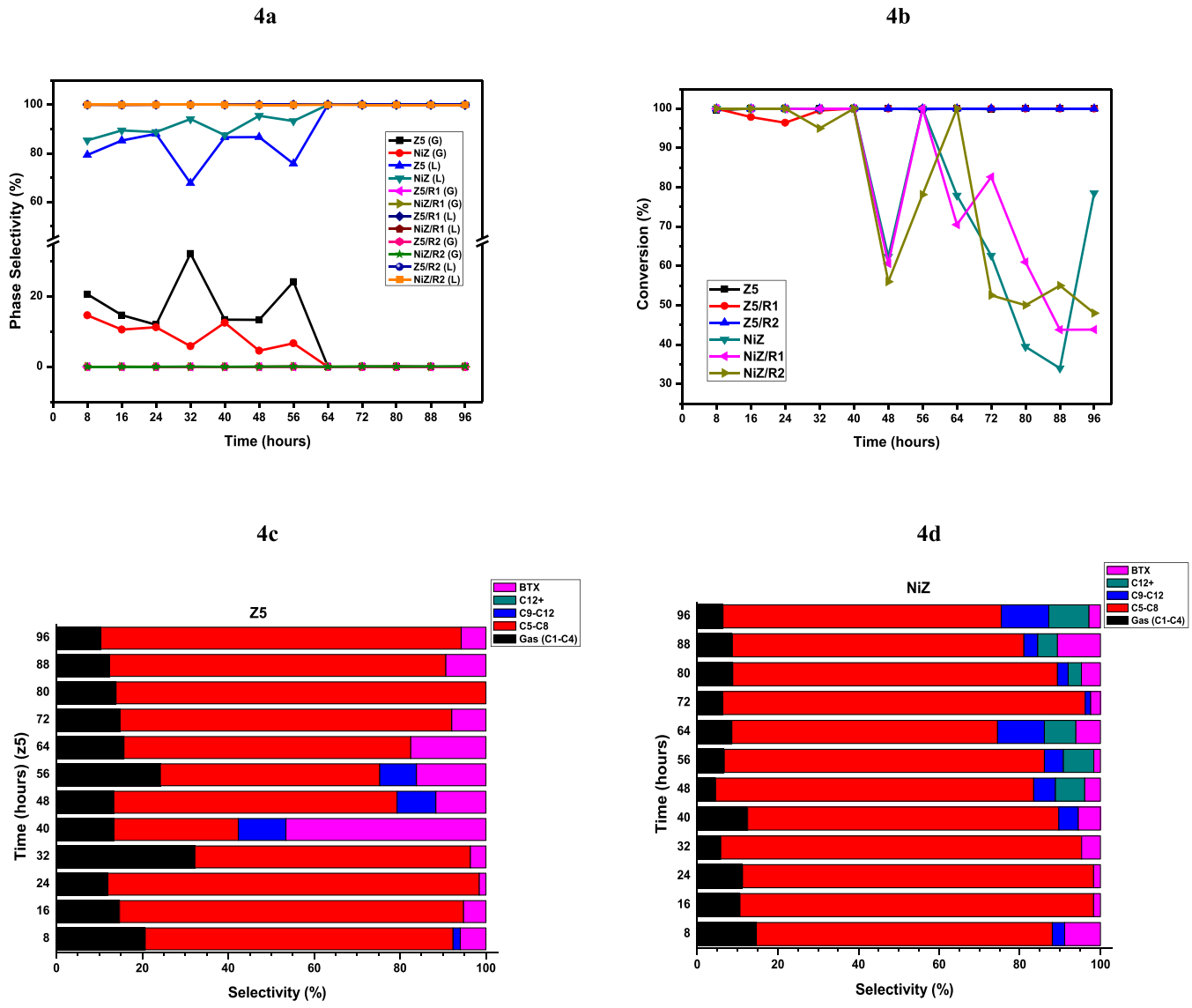

Fig. 4. Ethanol conversion and phase selectivity (a & b); Product distribution of Z5 and NiZ catalysts from first cycle (a & b), Z5-R1 and NiZ-R1 from 2nd cycle (b & c), Z5-R2 and NiZ-R2 from 3rd cycle ETH conversion at 623 K, 7 h^{-1} WHSV and 96-h TOS.

deactivation and a reduction in ethanol conversion. The unmodified catalyst, Z5, demonstrated considerable stability with a high ETH conversion of approximately 100% from 8 to 96 h on stream. The selectivity of this Z5 catalyst was significant for C_5-C_8 and BTX, while C_9-C_{12} HCs were more evident at the early stages of the reaction (8 h) and after 56 h on stream. For the Ni-doped catalyst, NiZ, the ETH conversion gradually decreased from 100% to 62.4% after 40 h on stream. This decrease in conversion can be attributed to the further oligomerisation of ethylene formed by ethanol dehydration in the early stages of the reaction [50]. Additionally, after 32 and 40 h on stream, the selectivities of the NiZ catalyst to C_5-C_8 and BTX decreased, respectively, shifting towards C_9-C_{12} and C_{12}+ selectivity. However, the ETH conversion rate gradually increased to approximately 100% at 56 h but then reduced to 39.5% after 80 h and later increased to 78.6% after 88 h on stream. The selectivity to C_5-C_8 showed a sharp increase after 64 h on stream, possibly due to the weakened strength of acid sites during deactivation.

For the Z5 catalyst, there appeared to be a correlation between BTX selectivity and C_5-C_8 selectivity and an inverse correlation between C_5-C_8 selectivity and C_{12}+ selectivity. This suggests that the Z5 catalyst is more selective to C_5-C_8, BTX, and a few C_9-C_{12} hydrocarbons, not favouring long-chain (C_{12}+) HCs. Gaseous HCs (C_1-C_4) decreased with increasing TOS, with a considerable decrease recorded after 64 h on stream for both catalysts (Fig. 4c). Compared to Z5, NiZ showed a wider product distribution, with a strong correlation between BTX and C_5-C_8 HCs due to their selectivity at all TOS and a weak correlation between C_9-C_{12} and C_{12}+ attributed to their selectivity after 40 h on stream (Fig. 4d). While both catalysts demonstrated considerable selectivity towards C_5-C_8 hydrocarbons, Z5 showed the highest selectivity towards C_5-C_8 (86.4%), C_9-C_{12} (11.1%), and BTX (46.6%) at 24, 40, and 40 h on stream, respectively. NiZ recorded the highest selectivity at 72, 96, 88, and 96 h on stream for C_5-C_8 (89.9%), C_9-C_{12} (11.8%), BTX (10.6%), and C_{12}+ (10%). Comparatively, Z5 showed higher (average) selectivity for C_1-C_4 (16.5%) and BTX (10.9%), while NiZ showed considerable (average) selectivity to C_5-C_8 (79.2%), C_9-C_{12} (4.1%), and C_{12}+ (4.5%) after the first cycle. This showed that the addition of Ni reduced the formation of BTX and gaseous hydrocarbons and increased the selectivity towards C_5+ hydrocarbons. Overall, the Z5 catalyst exhibited considerable stability than NiZ. However, NiZ showed a wider product distribution after the first cycle using the pure catalyst.

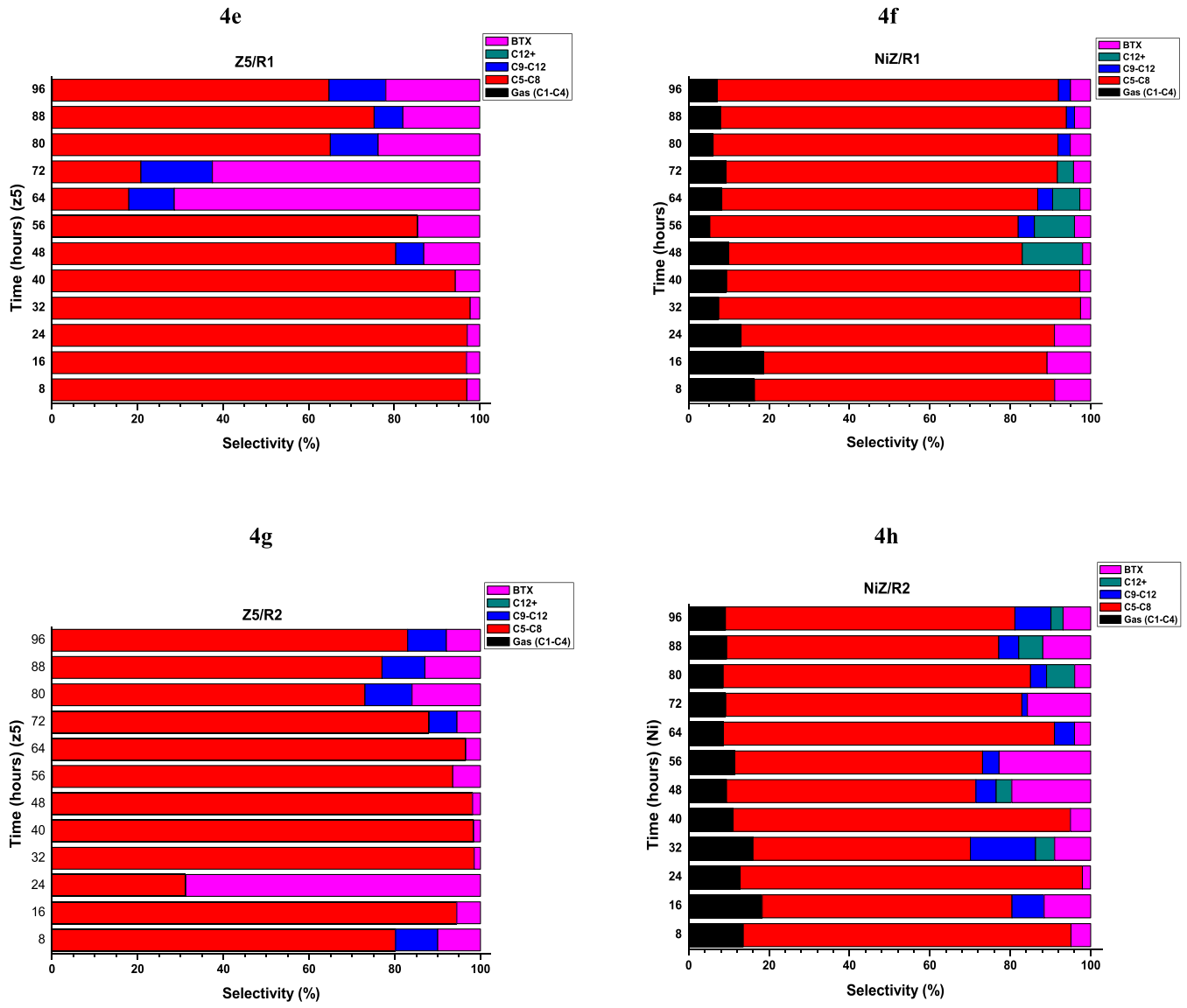

Fig. 4. (*continued*).

3.3. Catalyst regeneration and reusability study

Catalysts were subjected to a regeneration process under an airflow of 80 mL/min at a temperature of 823 K for 5 h after the first cycle. The results of the first regeneration process (R1) indicated an improvement in the catalytic performance of the spent and deactivated catalysts, particularly for the Ni-doped catalyst. The Z5-R1 catalysts, which had been regenerated, maintained an appreciable ETH conversion (>96%) and showed improved catalytic performance, especially with regard to (average) selectivity towards BTX (18.1%) and C_9-C_{12} (5.4%) (Fig. 4e). This was a substantial improvement from the Z5 catalyst, which recorded 10.9% and 2.5% for these HC fractions, respectively. Unlike Z5, the Z5-R1 catalyst showed increased C_9-C_{12} selectivity over time on stream, with the highest selectivity recorded at 72 h (16.7%). The selectivity towards BTX also increased with increasing time on stream and plateaued after 56 h at 55.4%, gradually declining to 53.5% at 72 h and then decreasing more rapidly afterwards. Like Z5, the Z5-R1 catalyst showed selectivity towards C_9-C_{12} after 40 h on stream and considerable selectivity towards C_5-C_8, with a dip in the latter at 64 and 72 h on stream attributed to a shift to BTX selectivity. The regenerated metal-doped catalyst, NiZ-R1, showed an improved catalytic activity after regeneration following the deactivation and a decrease in ETH conversion was observed in the first cycle after 96 h on stream. Yung, et al. [18] and Li, et al. [46] reported a similar trend. Like the pure NiZ, the NiZ-R1 catalyst exhibited a stable ETH conversion of approximately 100% up to 48 h on stream, where a decrease to 60.6% was recorded, followed by a continuous gradual decline after 56 h on stream (Fig. 4f). In contrast to NiZ, an increase in the production of C_5-C_8 (5.9% average increase in selectivity), resulting in a decrease in C_9-C_{12} and C_{12}+ selectivity, was observed with the NiZ-R1 catalyst. Both regenerated catalysts, Z5-R1 and NiZ-R1, showed a drastic reduction in selectivity towards gaseous HCs with increasing TOS. It can be deduced from the regeneration (R1) and application of regenerated catalysts that the catalysts retained their catalytic activity after the first regeneration cycle, which showed that the catalyst did not undergo irreversible dealumination during the long TOS in the ETH process [46,51]. The product distribution for the second cycle of ETH conversion showed that Z5-R1 favoured C_9-C_{12} and BTX, while NiZ-R1 was more preferential towards C_5-C_8 and slightly C_{12}+ HCs. This is similar to the product distribution for the first cycle, except that the NiZ catalyst was more selective towards C_9-C_{12} than Z5.

The results of the third cycle of ETH conversion using the second regeneration cycle catalysts Z5-R2 and NiZ-R2 are presented below. The operating conditions used were similar to those described in the

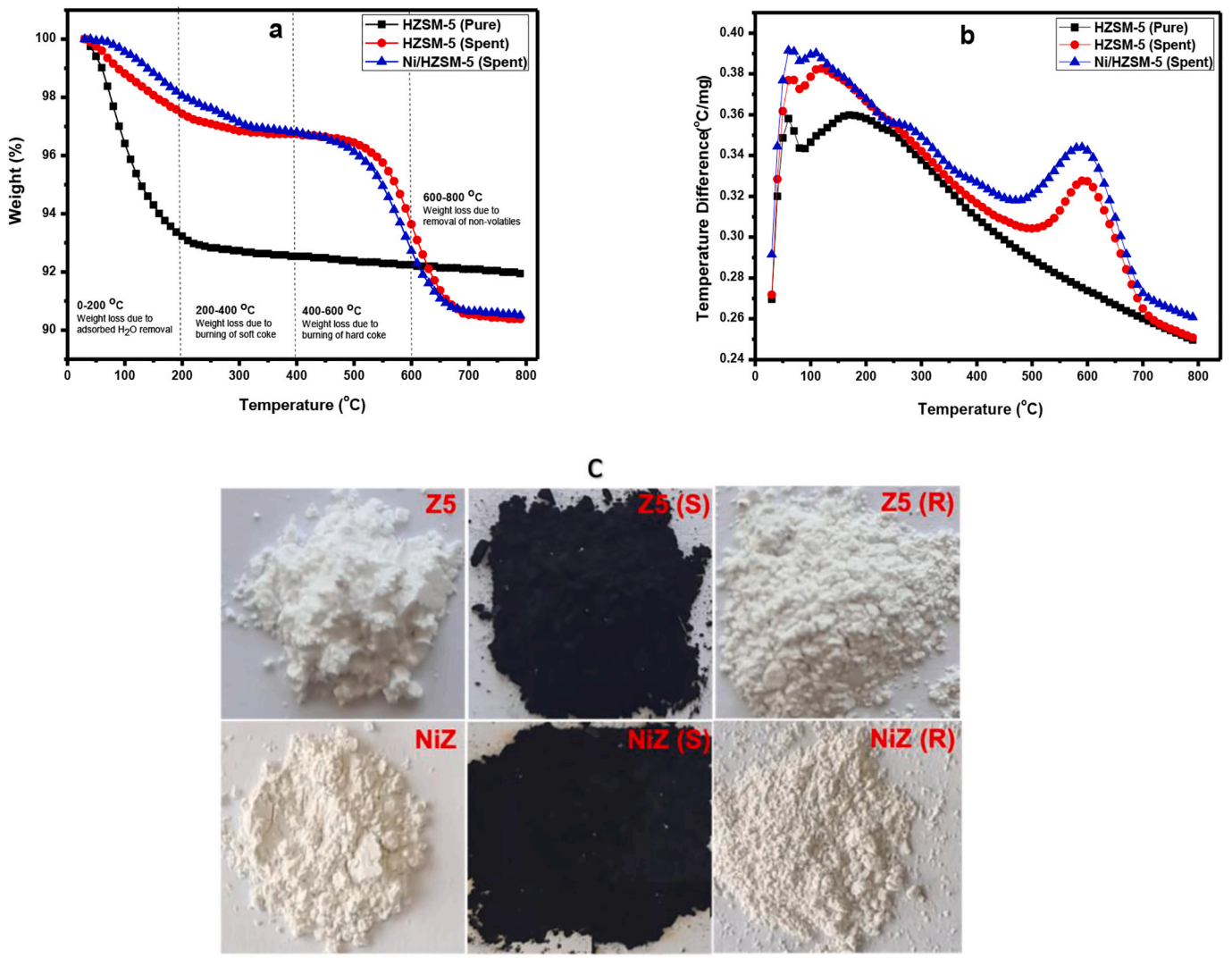

Fig. 5. (a & b). TGA-DTA of spent catalysts; (5c). Images of as-synthesised (Z5 and NiZ), spent (Z5 (S) and NiZ (S)) and regenerated (Z5 (R) and NiZ (R)) catalyst.

previous cycle. The results showed that the catalysts retained their activity at the same TOS as the pure catalysts. The Z5-R2 catalyst maintained 100% conversion up to 96 h on stream with the same selectivity to C_5-C_8, BTX, and slightly C_9-C_{12} without favouring C_{12}+ HCs. At 24 h on stream, the selectivity towards BTX showed a considerable increase with 50.8% selectivity, resulting in a decrease in C_5-C_8 selectivity (Fig. 4g). However, with an increase in TOS, the selectivity towards BTX experiences a drastic dip after 24 h on stream. As mentioned earlier, the selectivity towards C_5-C_8 was more prominent (>50% selectivity) except for 24 h on stream, while C_9-C_{12} was observed after 64 h. However, just like other catalysts, Z5-R1 and Z5, the Z5-R2 catalyst did not favour the synthesis of C_{12}+ HCs. However, the third cycle of ETH conversion using the regenerated NiZ-R2 exhibited an appreciable stable conversion like its other counterpart with >92% ETH conversion up to 48 h on stream, where a significant decrease to 52.9% was experienced. However, conversion increased to 70 and 100% afterwards at 56 and 64 h, respectively, before recording a continuous reduction till 96 h on stream. NiZ-R2 showed a wider product distribution similar to its other counterpart. However, compared to NiZ-R1, it recorded an average increase in selectivity for C_9-C_{12}, C_{12}+, and BTX by 3.8%, 1.5%, and 5.0%, respectively, after 96 h on the stream (Fig. 4h). From the second cycle of ETH conversion, it can be deduced that both catalysts (Z5-R2 and NiZ-R2) were more selective to liquid HCs (>83%), just like other catalysts evaluated. However, while the Z5-R2 catalyst was preferential to BTX with an average of 10.1%, NiZ-R2 favoured C_5-C_8, C_9-C_{12}, and C_{12}+ with 73.2%, 4.4%, and 2.1% selectivity, respectively, after 96 h time on stream. The catalytic evaluation of R2 catalysts in the third cycle of ETH conversion showed that the catalytic properties of the catalysts were restored after the regeneration process. The comparative review of the pure and regenerated catalyst is presented in Table 3.

Based on the results obtained from the experiment, it can be deduced that the as-synthesised novel catalyst, Z5, maintained considerable stability with ETH conversion of approximately 99.5% for three conversion cycles, each lasting for 96 h on stream each and even after two regeneration cycles. However, the deactivation of the metal-doped catalyst, NiZ catalyst, was not caused by dealumination or structural

Table 3
Comparative evaluation of product distribution (average) of pure and regenerated catalysts.

Catalysts	C_1-C_4 (%)	C_5-C_8 (%)	C_9-C_{12} (%)	C_{12}+ (%)	BTX (%)	X (%)	Liquid HC (%)
Z5	16.48	70.05	2.53	0.00	10.94	99.94	83.52
NiZ	8.76	79.23	4.07	3.40	4.53	79.57	91.24
Z5-R1	16.72	59.77	5.43	0.00	18.09	99.48	83.28
NiZ-R1	9.91	85.12	0.56	0.57	3.84	80.19	90.09
Z5-R2	16.77	69.08	3.86	0.00	10.29	100.00	83.23
NiZ-R2	11.48	73.21	4.40	2.05	8.86	73.41	88.52

distortion resulting from prolonged time on stream. Instead, this deactivation can be attributed to the formation of carbon deposits that block the active sites, leading to a decrease in ETH conversion. As a result, the employed regeneration technique proved to be highly effective in removing the coke deposits, thereby reviving the catalytic properties of the catalyst without damaging the structural framework. Furthermore, the application of the regenerated catalysts demonstrated that they all retained their catalytic performance after the regeneration process. However, it was observed that the unmodified catalyst exhibited more excellent stability than the Ni-doped catalyst, which can be attributed to the presence of Ni species in the NiZ catalyst. These species were found to increase coke formation and subsequent deactivation, thereby reducing the overall effectiveness of the catalyst.

ZSM-5 zeolite is a widely used catalyst in converting ethanol to fuels to valuable chemicals such as aromatics. It is believed that the initial rates of ethylene synthesis during ethanol dehydration and other secondary reactions via the direct and sequential routes are attributed to the active Bronsted acid and high Lewis acid sites in the as-synthesised catalysts [52]. Researchers argue that these active sites create a molecular constraint within the HZSM-5 channels, leading to a rate of diffusion that is less than that of production. Consequently, this helps with oligomerisation reactions of ethylene and other subsequent reactions [50,53,54]. Studies have revealed that the addition of transition metals like nickel in zeolite acid catalysts can enhance their catalytic performance. These transition metals help increase the total number of acid sites and improve the catalyst's selectivity towards specific products, making it more efficient in catalysing the conversion process [55–57] for improved (broader) product distribution, as demonstrated by the Ni-doped catalyst. However, the deactivation of ZSM-5 is a major challenge, which can significantly affect its catalytic performance and efficiency. The deactivation of ZSM-5 in ethanol conversion is caused by coke deposition. The use of transition metals while improving catalytic performance and product distribution has also been found to increase the tendency to coke deposition, leading to the blocking of catalyst pores and the subsequent deactivation of the catalyst, which results in a decline in catalytic performance and ethanol conversion [58,59].

The coke is formed due to the adsorption and polymerisation of the reaction intermediates on the catalyst surface, leading to pore blockage and reduced accessibility of the active sites. One of the main reasons for the deactivation of nickel-doped ZSM-5 compared to unmodified HZSM-5 is the poisoning of active sites by coke deposition [60–62]. During the reaction, the hydrocarbon molecules can undergo dehydrogenation, cracking, and polymerisation, forming carbonaceous species that adsorb on the catalyst surface and block the active sites. The deposition of coke is more pronounced in nickel-doped ZSM-5 due to the high activity of nickel towards the dehydrogenation reaction, which promotes the formation of carbonaceous species [63,64]. The stronger acid sites are more susceptible to coking, and this early deactivation of the catalyst is primarily caused by coke deposition on these sites [65]. The coke deposition can lead to a decrease in the surface area of the catalyst, reducing the accessibility of the reactants to the active sites and, therefore, decreasing the catalytic activity. Low-temperature coke (473 K) is usually olefinic or paraffinic, with species having >10 carbon atoms that cover these catalytic sites [66]. Coke produced at higher temperatures (>573 K), such as in the current investigation (623 K), is often more hydrogen deficient [67]. However, owing to the ability to regenerate the catalyst while maintaining its catalytic performance, it is believed that the deactivation of Ni-doped catalysts was not due to dealumination. Various factors, such as exposure to acids, bases, or high-temperature steam, can cause dealumination. Dealumination can result in a decrease in the catalyst's activity and selectivity and can be irreversible. Regeneration of dealuminated ZSM-5 catalysts can be challenging and may require complex treatments to reintroduce the lost acidic sites [68–70]. The catalysts used in this study were not exposed to high reaction temperatures (>823 K) or acidic media, making it possible to regenerate the spent catalysts.

Another factor that may partly contribute to the deactivation of nickel-doped ZSM-5 is the pore blockage by the nickel particles. The addition of nickel to ZSM-5 can lead to the formation of larger particles (as revealed by the PSD analysis) that can block the pores and channels of the zeolite, hindering the diffusion of the reactants and products. The blockage of the pores can also lead to a decrease in the surface area and acidity of the catalyst, reducing the catalytic activity [71,72]. The pore blockage is more pronounced in nickel-doped ZSM-5 due to the higher propensity of nickel to form larger particles than other metals, such as platinum or palladium [73]. The Ni-doped catalyst was more selective to long-chain HCs. Consequently, coke deposition on nickel-doped ZSM-5 can lead to a decrease in the selectivity towards long-chain hydrocarbons and an increase in coke generation, leading to catalyst deactivation. Furthermore, the sintering of the nickel particles can also contribute to the deactivation of the catalyst. During the reaction, the nickel particles can undergo agglomeration and sintering, decreasing the active surface area and the number of active sites. The sintering of the nickel particles is more pronounced at high temperatures or under oxidative conditions, which can lead to the migration and coalescence of the particles [74,75]. The sintering can be mitigated by controlling the reaction conditions or using a support material stabilising the nickel particles. However, in some cases, sintering may be irreversible and lead to a loss of catalyst activity and selectivity, ultimately requiring catalyst replacement.

On the contrary, some studies have reported that the addition of transition metals in the HZSM-5 catalyst has been shown to enhance its performance and stability in the conversion of ethanol into hydrocarbons. Doping these transition metals creates strong and stable acid sites in the catalyst, promoting catalytic activity and preventing the leaching of aluminium ions that can lead to catalyst deactivation. According to Kostyniuk, et al. [76], introducing some transition metals into the HZSM-5 zeolite improved the catalyst's hydrothermal stability and a higher aromatics yield. This behaviour was ascribed to the dehydrogenating activity of nickel and the moderate acidity strength brought about by the presence of the metal. The appreciable stability exhibited by the catalyst in the isomerisation of 1-hexene can be attributed to the bimetallic metal loading on the catalyst (denoted as Mo-Ni/HZSM-5) [76]. To overcome the deactivation challenge, monitoring and controlling the amount of coke produced during the catalytic reaction is crucial to maintain the catalyst's performance and prolong its lifespan. Therefore, the addition of transition metals to zeolite acid catalysts holds promise as a potential strategy to enhance their effectiveness in ethanol conversion, provided proper coke control and regeneration measures are implemented.

3.4. Assessing coke deposition on spent catalysts through TGA-DTA

Catalytic reactions involving hydrocarbons often result in the deposition of carbonaceous species, commonly referred to as coke, on the catalyst surface. Coke deposition is a major problem in the catalytic process, as it leads to catalyst deactivation and reduces its activity and selectivity. The coke deposition of HZSM-5 and nickel-doped HZSM-5 (Ni/HZSM-5) catalysts during ethanol conversion was studied.

The initial weight loss at 0–200 °C can be attributed to the removal of absorbed water and volatile compounds. HZSM-5 and Ni/HZSM-5 have a large surface area and can adsorb water and volatile compounds during ethanol conversion. Weight loss in this temperature range is to be expected and is not related to coke deposition. The HZSM-5 zeolite catalyst is known for its high acidity, which promotes coke deposition during ethanol conversion. The Z5 catalyst recorded a weight loss of 3.1 and 2.1 wt% at 200–400 °C and 400–600 °C (Fig. 2a) due to the combustion of soft and hard coke. This catalyst had more soft coke, which is relatively easy to burn at lower temperatures than hard coke. The coke deposition observed in Z5 catalysts is due to its high acidity, which promotes the cracking of ethanol into smaller molecules and favours coke formation. This also was reported by Xia, et al. [77]. The NiZ

catalyst, on the other hand, exhibited a more significant deposition of hard coke, up to 2.8 wt% and 2.5 wt% soft coke. The increased deposition of hard coke observed for the NiZ catalyst is attributed to nickel, which promotes coke formation and enhances the combustion of soft coke. This results in less soft coke accumulation on the catalyst surface and higher selectivity for long-chain hydrocarbons, as evidenced by a wider product distribution of the NiZ catalyst. The enhanced combustion of soft coke on the NiZ catalyst is due to the catalytic effect of nickel in the oxidation of coke. This catalytic effect is due to the large surface area of the NiZ catalyst and the redox properties of nickel [78]. In this case, soft coke formation is due to the accumulation of intermediates such as acetaldehyde on the catalyst surface, which form long-chain hydrocarbons and coke by further polymerisation, leading to the deactivation of the NiZ catalyst. To further support the findings of this study, it is worth noting that several other studies [79–81] have reported similar trends regarding high coke deposition on Ni-doped catalysts and their activity, further validating the results of our study. These findings suggest consistency in the behaviour of spent catalysts and reinforce the significance of coke deposition studies.

The pure (unused) HZSM-5 catalyst exhibited the least weight loss during the reaction because it was not exposed to the reactants, and no coke deposits occurred. However, the weight loss at 0–200 °C was high due to the removal of absorbed water and volatile compounds. The weight loss observed for spent catalysts (Z5 and NiZ) at 600–800 °C was due to the removal of non-volatile compounds from the ethanol conversion. The removal of non-volatile compounds is facilitated by high temperatures and an oxidative environment that promotes cracking and oxidation of these non-volatile heavier molecules absorbed at the catalyst surface during the reaction. The differential thermal analysis (DTA) curve showed a slightly higher peak for the NiZ catalyst, indicating a tendency towards coking (Fig. 2b). This is consistent with the heavy coke deposition observed for NiZ catalysts. Fig. 2c presents the images of spent and regenerated Z5 and NiZ catalysts.

From the coke deposition study, it can be inferred that the deactivation of the NiZ catalyst, which exhibits lower ethanol conversion after 48 h compared to the more stable Z5 catalyst, is partly due to the increased deposition of hard coke. This deactivation can also be attributed to nickel doping and increased selectivity for long-chain hydrocarbons. The increased selectivity for long-chain hydrocarbons in this catalyst is due to the decreased acidity and increased pore size due to the nickel doping. The reduced acidity leads to less cracking and condensation, forming long-chain hydrocarbons. The larger pore size allows the diffusion of larger molecules and reduces the accessibility of active sites, resulting in lower catalytic activity, faster deactivation, and lower ethanol conversion rate. Increased coke deposition on the NiZ catalyst also contributes to its faster deactivation, as it reduces the availability of active sites and increases the diffusion resistance of reactants and products.

4. Concluding remark

This study investigates the stability and regeneration of as-synthesised ZSM-5 zeolite catalyst in ethanol conversion into hydrocarbons at 623 K and 7 h-1 WHSV for 96 h on stream. Catalyst regeneration was conducted after 96 h on stream for two cycles. Product distribution revealed that aromatics, C_5-C_8, and C9+ hydrocarbons were the main liquid products, and their selectivity changed over time on stream. The Z5 catalyst maintained high-level stability in ethanol conversion, while the Ni-doped catalyst, NiZ, decreased conversion over time. Both catalysts showed selectivity towards C_5-C_8 hydrocarbons, but Z5 had higher selectivity for C_5-C_8 and BTX, while NiZ had higher selectivity for C_5-C_8, C_9-C_{12} and C_{12}+ hydrocarbons. Incorporating Ni reduced the formation of BTX and gaseous hydrocarbons and increased selectivity towards C_5+ HCs.

The regeneration process for both catalysts improved their catalytic performance, particularly for the Ni-doped catalyst. The Z5-R1 catalyst maintained a high ethanol conversion (>96%) and showed an increase in selectivity towards BTX (20.17%) and C_9-C_{12} (5.42%) compared to the as-synthesised Z5 catalyst. On the other hand, the NiZ-R1 catalyst exhibited stable ethanol conversion (~100%) up to 48 h on stream, with a decrease to 60.6% at 72 h and a considerable increase in selectivity towards C_5-C_8 hydrocarbons. Both regenerated catalysts showed a significant reduction in selectivity towards gaseous hydrocarbons, and their product distribution remained similar to the first cycle. The third cycle of ETH conversion using Z5-R2 and NiZ-R2 catalysts from the second regeneration cycle demonstrated that these catalysts retained their activity and product distribution up to the same time on stream as the as-synthesised catalysts. This suggests that the regeneration process successfully restored the catalytic properties of the catalysts. Z5-R2 catalyst maintained 100% conversion up to 96 h on stream, with selectivity to C_5-C_8, BTX, and slightly C_9-C_{12}. NiZ-R2 also exhibited stable conversion, with >92% ETH conversion up to 48 h on stream, before experiencing a significant decrease. Both catalysts were more selective to liquid HCs (> 99%). Z5-R2 catalyst was preferential to BTX, while NiZ-R2 favoured C_5-C_8, C_9-C_{12}, and C_{12}+. Overall, Z5 demonstrated greater stability than NiZ, while the regeneration process improved the catalytic activity of the spent and deactivated catalysts, indicating the potential for catalyst reuse and sustainability. Examination of the regenerated catalysts revealed that the structural and functional groups of the catalysts remained unchanged and the MFI framework and physiochemical properties were retained after 96 h TOS ETH conversion and the subsequent regeneration process. This confirms the ability of the regenerated catalysts to exhibit comparable catalytic performance to that of the pure catalysts. The NiZ catalyst showed higher coke deposition than the unmodified HZSM-5 catalyst. The nickel on the NiZ catalyst promotes coke formation and enhances its combustion, resulting in increased selectivity for long-chain hydrocarbons and faster deactivation.

The results of this study provided valuable insights into the stability and effectiveness of the as-synthesised catalysts, Z5 and NiZ, in ETH conversion. Specifically, it was observed that this catalyst (Z5) maintained a high level of stability, achieving an ETH conversion rate of approximately 100% for three conversion cycles, each lasting 96 h on stream. However, NiZ maintained stability up to 48 h on stream before gradually declining. This level of stability was maintained even after the catalyst underwent two regeneration cycles. The study of the regenerated catalysts showed that the applied regeneration method successfully preserved the textural and morphological properties of the catalyst while improving the catalytic performance. Understanding the coke deposition behaviour of HZSM-5 and Ni/HZSM-5 catalysts is critical for optimising the catalytic process and developing effective strategies to mitigate coke formation and deactivation. Such findings suggest that these catalysts may be attractive for industrial applications, where catalyst stability and longevity are crucial considerations. Overall, these results indicate that the catalysts could be a promising solution to address the challenges associated with ETH conversion, providing a stable and effective catalyst option for future use.

Funding

This work is financially supported by an international collaborative project (BRICS2019–040) under the BRICS STI Framework Programme with government funding organisations of South Africa NRF (BRIC190321424123), Brazil CNPq (402849/2019–1), Russia RFBR (19–58-80016), India DST (CRG/2018/004610, DST/TDT/ TDP-011/2017) and China MOST (2018YFE0183600).

Declaration of Competing Interest

None.

Data availability

Data will be made available on request.

Appendix A. Supplementary data

Supplementary data to this article can be found online at https://doi.org/10.1016/j.catcom.2023.106802.

References

[1] L. Zhang, C. Xu, P. Champagne, Overview of recent advances in thermo-chemical conversion of biomass, Energy Convers. Manag. 51 (5) (2010) 969–982, 2010/05/01/, https://doi.org/10.1016/j.enconman.2009.11.038.

[2] I.M.S. Anekwe, L. Khotseng, Y.M. Isa, The place of biofuel in sustainable living; prospects and challenges, in: Reference Module in Earth Systems and Environmental Sciences, Elsevier, 2021.

[3] R. Argauer, G. Landolt, US Pat., 3 702 886, 1972;; DM Bibby, NB Milestone and LP Aldridge, Nature 280 (1979) 664.

[4] R. Lago, et al., The nature of the catalytic sites in HZSM-5-activity enhancement, in: Studies in Surface Science and Catalysis vol. 28, Elsevier, 1986, pp. 677–684.

[5] M. Göhlich, W. Reschetilowski, S. Paasch, Spectroscopic study of phosphorus modified H-ZSM-5, Microporous Mesoporous Mater. 142 (1) (2011) 178–183.

[6] Z.S. Sousa, D.V. Cesar, C.A. Henriques, V.T. da Silva, Bioethanol conversion into hydrocarbons on HZSM-5 and HMCM-22 zeolites: use of in situ DRIFTS to elucidate the role of the acidity and of the pore structure over the coke formation and product distribution, Catal. Today 234 (2014) 182–191.

[7] E. Brunner, et al., Solid-state nmr and catalytic studies of mildly hydrothermally dealuminated HZSM-5, Zeolites 9 (4) (1989) 282–286.

[8] M. Seifert, et al., Ethanol to aromatics on modified H-ZSM-5 part I: interdependent dealumination actions, ChemCatChem 12 (24) (2020) 6301–6310, https://doi.org/10.1002/cctc.202001344.

[9] A.D. Chowdhury, A. Lucini Paioni, G.T. Whiting, D. Fu, M. Baldus, B. M. Weckhuysen, Unraveling the homologation reaction sequence of the zeolite-catalyzed ethanol-to-hydrocarbons process, Angew. Chem. Int. Ed. 58 (12) (2019) 3908–3912.

[10] K. Cumming, B.W. Wojciechowski, Hydrogen transfer, coke formation, and catalyst decay and their role in the chain mechanism of catalytic cracking, Catal. Rev. 38 (1) (1996) 101–157.

[11] K. Van der Borght, et al., Insights into the reaction mechanism of ethanol conversion into hydrocarbons on H-ZSM-5, Angew. Chem. Int. Ed. 55 (41) (2016) 12817–12821.

[12] K. Murata, M. Inaba, I. Takahara, Effects of surface modification of H-ZSM-5 catalysts on direct transformation of ethanol into lower olefins, J. Jpn. Pet. Inst. 51 (4) (2008) 234–239, https://doi.org/10.1627/jpi.51.234.

[13] N. Xue, et al., Understanding the enhancement of catalytic performance for olefin cracking: hydrothermally stable acids in P/HZSM-5, J. Catal. 248 (1) (2007) 20–28, https://doi.org/10.1016/j.jcat.2007.02.022.

[14] N. Xue, R. Olindo, J.A. Lercher, Impact of forming and modification with phosphoric acid on the acid sites of HZSM-5, J. Phys. Chem. C 114 (37) (2010) 15763–15770, https://doi.org/10.1021/jp106621d.

[15] J. Zhuang, et al., Solid-state MAS NMR studies on the hydrothermal stability of the zeolite catalysts for residual oil selective catalytic cracking, J. Catal. 228 (1) (2004) 234–242, https://doi.org/10.1016/j.jcat.2004.08.034.

[16] S.J. Jong, A.R. Pradhan, J.F. Wu, T.C. Tsai, S.B. Liu, On the regeneration of coked H-ZSM-5 catalysts, J. Catal. 174 (2) (1998) 210–218, https://doi.org/10.1006/jcat.1998.1971. Art no. Ca981971.

[17] M. Guisnet, P. Magnoux, Deactivation by coking of zeolite catalysts. Prevention of deactivation. Optimal conditions for regeneration, Catal. Today 36 (4) (1997) 477–483, https://doi.org/10.1016/S0920-5861(96)00238-6.

[18] M.M. Yung, et al., Restoring ZSM-5 performance for catalytic fast pyrolysis of biomass: effect of regeneration temperature, Catal. Today 323 (2019) 76–85, 2019/02/15/, https://doi.org/10.1016/j.cattod.2018.06.025.

[19] P.L. Benito, A.T. Aguayo, A.G. Gayubo, J. Bilbao, Catalyst equilibration for transformation of methanol into hydrocarbons by reaction-regeneration cycles, Ind. Eng. Chem. Res. 35 (7) (1996) 2177–2182, https://doi.org/10.1021/ie950493u.

[20] T.R. Carlson, Y.T. Cheng, J. Jae, G.W. Huber, Production of green aromatics and olefins by catalytic fast pyrolysis of wood sawdust, Energy Environ. Sci. 4 (1) (2011) 145–161, https://doi.org/10.1039/c0ee00341g.

[21] V. Paasikallio, C. Lindfors, J. Lehto, A. Oasmaa, M. Reinikainen, Short vapour residence time catalytic pyrolysis of spruce sawdust in a bubbling fluidized-bed reactor with HZSM-5 catalysts, Top. Catal. 56 (2013) 800–812, https://doi.org/10.1007/s11244-013-0037-y, 9–10 ed. [Online]. Available, https://www.scopus.com/inward/record.uri?eid=2-s2.0-84879864781&doi=10.1007%2fs11244-013-0037-y&partnerID=40&md5=f6c9628624fe8f0e409f47eb4abda310.

[22] P.T. Williams, P.A. Horne, The influence of catalyst regeneration on the composition of zeolite-upgraded biomass pyrolysis oils, Fuel 74 (12) (1995) 1839–1851, https://doi.org/10.1016/0016-2361(95)80017-C.

[23] I.M.S. Anekwe, B. Oboirien, Y.M. Isa, Catalytic conversion of bioethanol over cobalt and nickel-doped HZSM-5 zeolite catalysts, Biofuels Bioprod. Biorefin. (2023) 1–15, https://doi.org/10.1002/bbb.2536.

[24] Y. Sun, et al., The influence of zoned Al distribution of ZSM-5 zeolite on the reactivity of hexane cracking, Mol. Catal. 484 (2020) 110770, 2020/03/01/, https://doi.org/10.1016/j.mcat.2020.110770.

[25] C.-J. Liu, Energy-efficient routes of fabricating thermoelectric materials, in: Handbook of Greener Synthesis of Nanomaterials and Compounds, Elsevier, 2021, pp. 521–548.

[26] G. Vezzalini, S. Quartieri, E. Galli, A. Alberti, G. Cruciani, A. Kvick, Crystal structure of the zeolite mutinaite, the natural analog of ZSM-5, Zeolites 19 (5–6) (1997) 323–325.

[27] G. Reding, T. Mäurer, B. Kraushaar-Czarnetzki, Comparing synthesis routes to nano-crystalline zeolite ZSM-5, Microporous Mesoporous Mater. 57 (1) (2003) 83–92.

[28] M. Yang, et al., Conversion of lignin into light olefins and aromatics over Fe/ZSM-5 catalytic fast pyrolysis: significance of Fe contents and temperature, J. Anal. Appl. Pyrolysis 137 (2019) 259–265.

[29] Y. Peng, et al., Fe-ZSM-5 supported palladium nanoparticles as an efficient catalyst for toluene abatement, Catal. Today 332 (2019) 195–200.

[30] D.T. Sarve, S.K. Singh, J.D. Ekhe, Ethanol dehydration to diethyl ether over ZSM-5 and β-Zeolite supported NiW catalyst, Inorg. Chem. Commun. 139 (2022) 109397, 2022/05/01/, https://doi.org/10.1016/j.inoche.2022.109397.

[31] G. Qi, R.T. Yang, Ultra-active Fe/ZSM-5 catalyst for selective catalytic reduction of nitric oxide with ammonia, Appl. Catal. B Environ. 60 (1–2) (2005) 13–22.

[32] G. Liu, F. Xiangli, W. Wei, S. Liu, W. Jin, Improved performance of PDMS/ceramic composite pervaporation membranes by ZSM-5 homogeneously dispersed in PDMS via a surface graft/coating approach, Chem. Eng. J. 174 (2–3) (2011) 495–503.

[33] E.M. Flanigen, H. Khatami, H.A. Szymanski, Infrared Structural Studies of Zeolite Frameworks, ACS Publications, 1971.

[34] H. Feng, C. Li, H. Shan, In-situ synthesis and catalytic activity of ZSM-5 zeolite, Appl. Clay Sci. 42 (3) (2009) 439–445, 2009/01/01/, https://doi.org/10.1016/j.clay.2008.05.004.

[35] R. Kachangoon, J. Vichapong, Y. Santaladchaiyakit, R. Burakham, S. Srijaranai, An eco-friendly hydrophobic deep eutectic solvent-based dispersive liquid–liquid microextraction for the determination of neonicotinoid insecticide residues in water, soil and egg yolk samples, Molecules 25 (12) (2020) 2785.

[36] B. Ba Mohammed, et al., Fe-ZSM-5 zeolite for efficient removal of basic Fuchsin dye from aqueous solutions: synthesis, characterization and adsorption process optimization using BBD-RSM modeling, J. Environ. Chem. Eng. 8 (5) (2020) 104419, 2020/10/01/, https://doi.org/10.1016/j.jece.2020.104419.

[37] X. Niu, J. Li, L. Zhang, Z. Lei, X. Zhao, C. Yang, ZSM-5 functionalized in situ with manganese ions for the catalytic oxidation of cyclohexane, RSC Adv. 7 (80) (2017) 50619–50625.

[38] A. Straß-Eifert, T.L. Sheppard, C.D. Damsgaard, J.-D. Grunwaldt, R. Güttel, Stability of cobalt particles in and outside HZSM-5 under CO hydrogenation conditions studied by ex situ and in situ electron microscopy, ChemCatChem 13 (2) (2021) 718–729, 2021/01/20, https://doi.org/10.1002/cctc.202001533.

[39] L. Heermann, D.L. DeAngelis, J. Borcherding, A new mechanistic approach for the further development of a population with established size bimodality, PLoS One 12 (6) (2017), e0179339.

[40] J. Niu, P. Rasmussen, R. Magee, G. Nilsson, Spatial and temporal variability of incidental nanoparticles in indoor workplaces: impact on the characterization of point source exposures, Environ Sci Process Impacts 17 (2014), https://doi.org/10.1039/c4em00478g, 11/20.

[41] B. Li, X. Lin, Y. Luo, X. Yuan, X. Wang, Design of active and stable bimodal nickel catalysts for methane reforming with CO2, Fuel Process. Technol. 176 (2018) 153–166.

[42] Z. Li, et al., Towards the preparation of binderless ZSM-5 zeolite catalysts: the crucial role of silanol nests, Cat. Sci. Technol. 10 (23) (2020) 7829–7841.

[43] N. Chu, et al., An unusual hierarchical ZSM-5 microsphere with good catalytic performance in methane dehydroaromatization, Microporous Mesoporous Mater. 118 (1) (2009) 169–175, 2009/02/01/, https://doi.org/10.1016/j.micromeso.2008.08.048.

[44] F. Rahmani, M. Haghighi, Y. Vafaeian, P. Estifaee, Hydrogen production via CO2 reforming of methane over ZrO2-Doped Ni/ZSM-5 nanostructured catalyst prepared by ultrasound assisted sequential impregnation method, J. Power Sources 272 (2014) 816–827, 2014/12/25/, https://doi.org/10.1016/j.jpowsour.2014.08.123.

[45] A. López, I. De Marco, B. Caballero, A. Adrados, M. Laresgoiti, Deactivation and regeneration of ZSM-5 zeolite in catalytic pyrolysis of plastic wastes, Waste Manag. 31 (8) (2011) 1852–1858.

[46] Y. Li, D. Yellezuome, C. Li, R. Liu, Deactivation mechanism and regeneration effect of bi-metallic Fe-Ni/ZSM-5 catalyst during biomass catalytic pyrolysis, Fuel 312 (2022) 122924.

[47] R.C. Deka, Acidity in Zeolites and their Characterization by Different Spectroscopic Methods, 1998.

[48] A. Aho, et al., Catalytic upgrading of woody biomass derived pyrolysis vapours over iron modified zeolites in a dual-fluidized bed reactor, Fuel 89 (8) (2010) 1992–2000.

[49] Z.Y. Zakaria, J. Linnekoski, N.A.S. Amin, Catalyst screening for conversion of glycerol to light olefins, Chem. Eng. J. 207-208 (2012) 803–813, https://doi.org/10.1016/j.cej.2012.07.072.

[50] M. Guisnet, P. Magnoux, Fundamental description of deactivation and regeneration of acid zeolites, in: Studies in Surface Science and Catalysis vol. 88, Elsevier, 1994, pp. 53–68.

[51] J. Wang, B.-C. Lin, Q.-X. Huang, Z.-Y. Ma, Y. Chi, J.-H. Yan, Aromatic hydrocarbon production and catalyst regeneration in pyrolysis of oily sludge using ZSM-5 zeolites as catalysts, Energy Fuel 31 (11) (2017) 11681–11689.

[52] J. Sun, Y. Wang, Recent advances in catalytic conversion of ethanol to chemicals, ACS Catal. 4 (4) (2014) 1078–1090.
[53] B. Ali, X. Lan, M.T. Arslan, S.Z.A. Gilani, H. Wang, T. Wang, Controlling the selectivity and deactivation of H-ZSM-5 by tuning b-axis channel length for glycerol dehydration to acrolein, J. Ind. Eng. Chem. 88 (2020) 127–136.
[54] A.T. Aguayo, A.G. Gayubo, J. Ereña, M. Olazar, J.M. Arandes, J. Bilbao, Isotherms of chemical adsorption of bases on solid catalysts for acidity measurement, J. Chem. Technol. Biotechnol. 60 (2) (1994) 141–146.
[55] E.F. Iliopoulou, S. Stefanidis, K. Kalogiannis, A. Delimitis, A. Lappas, K. Triantafyllidis, Catalytic upgrading of biomass pyrolysis vapors using transition metal-modified ZSM-5 zeolite, Appl. Catal. B Environ. 127 (2012) 281–290.
[56] Y.-L. Ding, H.-Q. Wang, M. Xiang, P. Yu, R.-Q. Li, Q.-P. Ke, The effect of Ni-ZSM-5 catalysts on catalytic pyrolysis and hydro-pyrolysis of biomass, Front. Chem. 8 (2020) 790.
[57] K. Van der Borght, V. Galvita, B. Marin, Ethanol to higher hydrocarbons over Ni, Ga, Fe-modified ZSM-5: effect of metal content, Appl. Catal. A Gen. 492 (2015) 02/25, https://doi.org/10.1016/j.apcata.2014.12.020.
[58] M. Rostamizadeh, F. Yaripour, H. Hazrati, Ni-doped high silica HZSM-5 zeolite (Si/Al= 200) nanocatalyst for the selective production of olefins from methanol, J. Anal. Appl. Pyrolysis 132 (2018) 1–10.
[59] A. Maia, B. Louis, Y. Lam, M. Pereira, Ni-ZSM-5 catalysts: Detailed characterization of metal sites for proper catalyst design, J. Catal. 269 (1) (2010) 103–109.
[60] Q. Li, Z. Sui, X. Zhou, Y. Zhu, J. Zhou, D. Chen, Coke formation on Pt–Sn/Al 2 O 3 catalyst in propane dehydrogenation: coke characterization and kinetic study, Top. Catal. 54 (2011) 888–896.
[61] T.A. Abdullah, Catalytic Conversion of Methanol to Hydrocarbons over different wt % Ni-HZSM-5, 2023.
[62] S. Du, D.P. Gamliel, M.V. Giotto, J.A. Valla, G.M. Bollas, Coke formation of model compounds relevant to pyrolysis bio-oil over ZSM-5, Appl. Catal. A Gen. 513 (2016) 67–81.
[63] S. Pinjari, et al., Maximizing the production of hydrogen and carbon nanotubes: effect of Ni and reaction temperature, Int. J. Hydrog. Energy 43 (5) (2018) 2781–2793.
[64] A. Maia, B. Oliveira, P. Esteves, B. Louis, Y. Lam, M. Pereira, Isobutane and n-butane cracking on Ni-ZSM-5 catalyst: effect on light olefin formation, Appl. Catal. A Gen. 403 (1–2) (2011) 58–64.
[65] S. Tabak, S. Yurchak, Conversion of methanol over ZSM-5 to fuels and chemicals, Catal. Today 6 (3) (1990) 307–327.
[66] H.G. Karge, J. Weitkamp, Zeolites as Catalysts, Sorbents and Detergent Builders: Applications and Innovations, Elsevier, 1989.
[67] C.B. Phillips, R. Datta, Production of ethylene from hydrous ethanol on H-ZSM-5 under mild conditions, Ind. Eng. Chem. Res. 36 (11) (1997) 4466–4475.
[68] P.K. Roy, R. Prins, G.D. Pirngruber, The effect of pretreatment on the reactivity of Fe-ZSM-5 catalysts for N2O decomposition: dehydroxylation vs. steaming, Appl. Catal. B Environ. 80 (3–4) (2008) 226–236.
[69] W. Zhang, X. Han, X. Liu, X. Bao, Characterization of the acid sites in dealuminated nanosized HZSM-5 zeolite with the probe molecule trimethylphosphine, J. Mol. Catal. A Chem. 194 (1–2) (2003) 107–113.
[70] M. Ibáñez, et al., Simultaneous coking and dealumination of zeolite H-ZSM-5 during the transformation of chloromethane into olefins, Cat. Sci. Technol. 6 (1) (2016) 296–306.
[71] K.M. Mlimi, Metal Modified Mesoporous ZSM-5 as Catalysts for the Oligomerization of 1-Hexene, 2021.
[72] Z. Wan, G.K. Li, C. Wang, H. Yang, D. Zhang, Relating coke formation and characteristics to deactivation of ZSM-5 zeolite in methanol to gasoline conversion, Appl. Catal. A Gen. 549 (2018) 141–151, 2018/01/05/, https://doi.org/10.1016/j.apcata.2017.09.035.
[73] A. Masalska, Ni-loaded catalyst containing ZSM-5 zeolite for toluene hydrogenation, Appl. Catal. A Gen. 294 (2) (2005) 260–272.
[74] B. Sarkar, R. Goyal, C. Pendem, T. Sasaki, R. Bal, Highly nanodispersed Gd-doped Ni/ZSM-5 catalyst for enhanced carbon-resistant dry reforming of methane, J. Mol. Catal. A Chem. 424 (2016) 17–26.
[75] Y. Liu, L. Liu, X. Diao, J. Liang, C. Wu, Y. Sun, Effective catalytic steam reforming of naphthalene over Ni-modified ZSM-5 via one-pot hydrothermal synthesis, Waste Manag. 147 (2022) 1–9.
[76] A. Kostyniuk, D. Key, M. Mdleleni, 1-hexene isomerization over bimetallic M-Mo-ZSM-5 (M: Fe, Co, Ni) zeolite catalysts: effects of transition metals addition on the catalytic performance, J. Energy Inst. 93 (2) (2020) 552–564, 2020/04/01/, https://doi.org/10.1016/j.joei.2019.06.009.
[77] W. Xia, et al., Multiple important roles of phosphorus modification on the ZSM-5 in ethanol to olefin reaction: Acidity adjustment, hydrothermal stability and anti-coking, Fuel 341 (2023), 127675.
[78] S. Kawi, Y. Kathiraser, J. Ni, U. Oemar, Z. Li, E.T. Saw, Progress in synthesis of highly active and stable nickel-based catalysts for carbon dioxide reforming of methane, ChemSusChem 8 (21) (2015) 3556–3575.
[79] Y. Li, et al., Coke formation on the surface of Ni/HZSM-5 and Ni-Cu/HZSM-5 catalysts during bio-oil hydrodeoxygenation, Fuel 189 (2017) 23–31.
[80] H.O. Mohamed, et al., Stable and reusable hierarchical ZSM-5 zeolite with superior performance for olefin oligomerization when partially coked, Appl. Catal. B Environ. 316 (2022) 121582.
[81] H.K.G. Singh, et al., Biogasoline production from linoleic acid via catalytic cracking over nickel and copper-doped ZSM-5 catalysts, Environ. Res. 186 (2020) 109616.